Analytical coupling detection in the presence of noise and nonlinearity

Theoden I. Netoff,[1,2] Louis M. Pecora,[3] and Steven J. Schiff[1,2,4,*]

[1]*Krasnow Institute for Advanced Studies, George Mason University, Fairfax, Virginia 22030, USA*
[2]*Program in Neuroscience, The George Washington University School of Medicine, Washington, DC 20037, USA*
[3]*Naval Research Laboratory, Washington, DC 20376 USA*
[4]*Department of Psychology, George Mason University, Fairfax, Virginia, 22030, USA*

A rigorous analytical approach is developed to test for the existence of a continuous nonlinear functional relationship between systems. We compare the application of this nonlinear local technique to the existing analytical linear global approach in the setting of increasing additive noise. For natural systems with unknown levels of noise and nonlinearity, we propose a general framework for detecting coupling. Lastly, we demonstrate the applicability of this method to detect coupling between simultaneous, experimentally measured, intracellular voltages between neurons within a mammalian neuronal network.

PACS number(s): 05.45.Tp, 87.10.+e, 87.17.Nn, 05.40.Ca

Faced with an experimental system whose equations are unknown, it is often important to determine when components of the system are coupled. An example of current interest is the behavior of neural systems. We now understand that many neural cognitive phenomena, from insects [1] to mammals [2], correspond to computations performed in transiently synchronous ensembles of neurons. But in order to define such functional ensembles, one must first determine whether the neurons are coupled.

Neural systems are examples of natural systems where the elements are highly nonlinear, and beset with an indeterminate amount of noise. We expect that all natural systems will present two types of impediments to detection of coupling: noise and nonlinearity. We introduce here the idea that there are two approaches to coupling detection, each of which are well suited to particular balances of noise and nonlinearity. If the balance is unknown, neither approach alone can be relied upon to detect coupling.

Cross correlation and continuity are examples of statistics suited to extreme cases of the balance between noise and nonlinearity. For instance, cross correlation probes globally for the simplest functional relation, linear, and is the most tolerant to noise. Noise tolerance comes from the linear nature of the assumed functional form which allows added noise to separate from the signal and average to zero. Cross correlation is well developed, and analytic estimates of significance for the statistic exist [3] obviating the need for bootstrap numerical testing [4]. Figure 1 schematically illustrates our present view of coupling detection. Unfortunately, in many experimental situations we do not know which quadrant from Fig. 1 is appropriate.

Continuity makes few assumptions about the nature of an underlying functional relationship, asking only whether a small region of data about a system state point from one system maps to a corresponding small region about a similar system state point in another system [5,6]. Continuity is thus a local property requiring minimal knowledge of the local structure of a function (e.g., no Jacobian must be accurately

fit [7]). Nonlinear measures of synchronization and prediction have recently been developed, which are capable of detecting coupling between nonlinear systems when linear methods fail. Previous work with spinal cord motoneurons were consistent with the usefulness of nonlinear methods to identify certain neuronal interactions [8]. Nevertheless, a continuity measure underlies many of the recent approaches, including prediction at zero time, mutual nearest neighbors, and mutual variance [8,9]. Importantly, continuity is an asymmetric property, and can be implemented to distinguish directionality of coupling [5].

We show here that, like cross correlation, we can put a continuity statistic and its associated significance in an analytical setting that eliminates the need for extensive numerical work to support the results. Previous attempts to quantify such measures have not dealt with the independence of sampled neighborhoods rigorously [5], or have resorted to bootstrap methods in order to establish the significance of continuity [8].

The continuity of a function relating multivariate data sets X and Y is quantified using local measures of continuity about selected fiduciary points x_i. The multivariate data can be simultaneous measurements of several variables or, in our examples, delay reconstructions from time series. Within a distance δ from x_i we can collect the n_i^{δ} nearest neighbors to
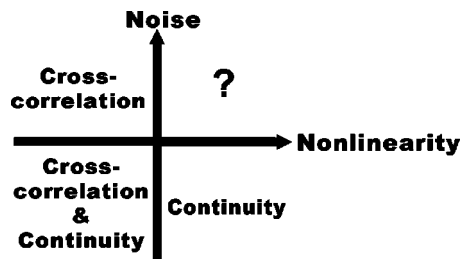

FIG. 1. Schematic of balance of noise vs nonlinearity, and optimal coupling detection schemes. In low noise, nonlinear methods have an advantage over linear methods for nonlinear systems. Linear methods are well suited to noisy linear systems. It is unknown how noise affects detection for highly nonlinear systems. For data from many natural systems, the quadrant is unknown *a priori*.

*Corresponding author; Email address: sschiff@gmu.edu

x_i. The x_i point has a corresponding time indexed point y_i in the Y data set. Within a distance ϵ from y_i will be n_i^ϵ nearest neighbors of y_i. For each fiducial point pair (x_i, y_i), a count m_i of the subset of n_i^δ points that have corresponding time indexed points within n_i^ϵ are determined.

Under the null hypothesis that there is no functional relationship between the two data sets, the nearest neighbors in δ will be no more likely to map into ϵ than if they had been chosen randomly from X. This can be thought of as a classic "urn" problem [10], where all of the points in the δ set are red and the rest of the X points are blue. If a continuous function exists relating X and Y, given an ϵ there will always be a δ where all red points are within ϵ. Since we are dealing with real data rather than analytical functions, we relax the strict definition and allow $m_i \leqslant n_i^\delta$ to be the number of red balls in the ϵ set.

Under the null hypothesis, points are randomly mapped from X to Y, and a handful n_i^ϵ are selected from Y without replacement. The number of m_i points in n_i^ϵ should therefore fall under the hypergeometric distribution $h(k|n_\delta, n_\epsilon, N) = \binom{n_\delta}{k}\binom{N-n_\delta}{n_\epsilon - k}/\binom{N}{n_\epsilon}$ [10], where $\binom{A}{B}$ is the binomial coefficient. The probability that k points from n_i^δ map into ϵ is equal to the number of combinations of k points that could have mapped into ϵ, $\binom{n_\delta}{k}$, multiplied by the number of combinations of points from outside δ that could have mapped into ϵ, $\binom{N-n_\delta}{n_\epsilon - k}$, divided by the total number of combinations of n_i^ϵ points that could have been selected, $\binom{N}{n_\epsilon}$.

We want to estimate the probability that m_i or fewer points from δ map into ϵ by chance. This probability is the sum of the cumulative hypergeometric function for $k = 0, \ldots, m_i$ $h_{cum}(m|n_\delta, n_\epsilon, N) = \sum_{k=0}^{m_i} h(k|n_\delta, n_\epsilon, N)$.

We define significant fiduciary points as those where h_{cum} suggests that m_i are significant. Global continuity is then evaluated by counting the number of significant fiduciary points, N_{sig}. The significance limit may be estimated by $m_* = \min\{m_i | h_{cum}(m_i|n_\delta, n_\epsilon, N) > 0.95\}$ (for fixed n_δ and n_ϵ), which sets a threshold m_*, the probability of which is the smallest integer value for which m_i is expected to occur with probability greater than 0.95. For a given m_* the corresponding $p_* = \mathrm{P}(m_i > m_*) = 1 - h_{cum}(m_*|n_\delta, n_\epsilon, N)$ is the probability that more points than m_* will map from δ into ϵ, which will be less than probability 0.05. The count of the number of fiducial points at which $m_i > m_*$ we call N_{sig}. To quantify the significance of the global continuity, we use the cumulative binomial distribution to determine the probability that the number of points that reached significance, N_{sig}, might have done so at random [10], $b_{cum}(N_{sig}|N_f, p_*) = \sum_{r=0}^{N_{sig}} [N_f!/r!(N_f-r)!]p_*^r(1-p_*)^{N_f-r}$, using the given p_* and N_f (number of fiducial points). If the cumulative binomial statistic is larger than 0.95, then we can reject our null hypothesis that the two data sets are uncoupled.

Using the hypergeometric function and the binomial distribution assumes that the fiduciary points and their neighbors must be independent, implying that the local neighborhoods cannot overlap. Overlapping the neighborhoods around the fiduciary points would result in larger numbers of

significant fiduciary points than would be anticipated by the binomial statistic. To prevent overlap the state space is tessellated into regions with equal numbers of points. Tessellation is performed by finding the first principal component of the entire data set (the direction for which most variance in the data is observed), projecting and rank ordering the points onto the first principal component, and tesselating the data set at the median point. Each of the two resulting regions are then similarly tessellated by finding the first principal components of each region and subdividing at their medians. The fiducial points were selected as the points closest to the geometric center of each tessellation. The method is therefore independent of inhomogeneities in the geometrical distribution of points.

Such a measure of continuity is dependent upon the selection of neighborhood sizes n^δ and n^ϵ. Without *a priori* knowledge of the data set's underlying dynamics or noise, a range of n^δ and n^ϵ are examined for a range of embedding dimensions.

Unidirectionally coupled Hénon maps were used to test the sensitivity of the continuity measure: $Y(t+1) = 1.4 - Y(t)^2 + 0.3Y(t-1), X(t+1) = 1.4 - [CY(t) + (1-C)X(t)]X(t) + 0.3X(t-1)$, where C sets the coupling strength. The top panel of Fig. 2 shows raw data for weak coupling, $C = 0.02$, after discarding the first 1000 transient points were discarded and the subsequent 8000 iterations used for analysis (top panel, Fig. 2). The second panel shows cross correlation with the Bartlet estimator [3] indicated as a 95% confidence limit (second panel). One would expect no more than 5% of the cross correlation values to be greater than this confidence interval by chance, and the data in this figure suggest no significant linear cross correlation.

The next panels in Fig. 2 illustrate how a small region of points labeled δ in the drive system (third panel left) maps to the correspondingly indexed points in the response system (third panel right). The tessellation of the Hénon system is illustrated in the driver data (third panel left of Fig. 2). Such tessellation was applied to the drive system until seven points remained within each tessellation, following which the most central points within the drive system were selected as fiducial, and the corresponding time indexed points in the response system were identified as fiducial. The ϵ regions of the response system were selected as nearest neighbors about these response fiducial points. The probabilities associated with both forward drive-to-response and reverse response-to-drive mappings were determined, by alternately selecting the driver or response system to be tessellated.

The bottom panel of Fig. 2 illustrates the result of the continuity statistic. Significant continuity is not identified for the drive-to-response system, as anticipated in the weak coupling regime. Nevertheless, there is significant continuity identified from the response to the drive system. In a unidirectional drive-response system, the response system at all finite coupling strengths always contains information and a significant mapping from response to drive. In such systems, the appearance of a functional relationship from drive to response is seen only at higher coupling strengths at the onset of generalized synchronization.
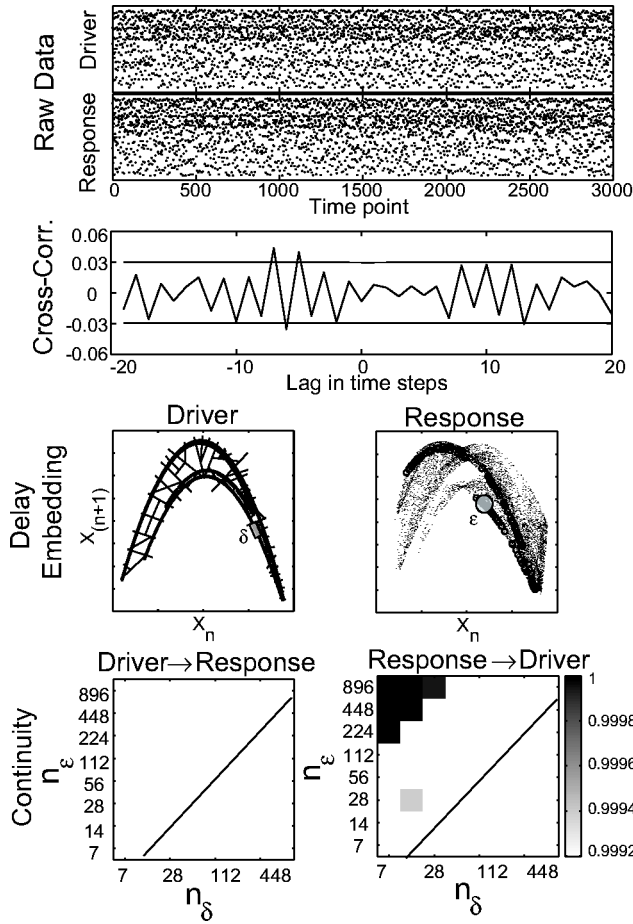
FIG. 2. Weakly coupled Hénon systems, with raw data from drive and response time series in upper panel. Second panel shows cross correlation, with 95% confidence intervals (Bartlett) indicated as solid lines. Third panel shows tessellation of driver Hénon system, and a δ region is indicated. Points from the δ region mapped to dark circles within the response system (right), and a fraction of these points fall within the ϵ region indicated. Lower panel shows continuity results with probability indicated as gray scale, dark being highly significant. Since we perform 64 separate comparisons for eight levels of δ and ϵ, we set the joint probability that none of the 64 comparisons were significant at $0.95 = (0.9992)^{64}$. We assume that ϵ will in general be larger than δ, and therefore only calculate values above the diagonal line.

The response of these two methods, cross correlation and continuity, as a function of additive noise is instructive. Figure 3 shows a comparison of sensitivity of the methods on coupled Hénon maps with four levels of Gaussian additive noise: 0, 0.125, 0.25, and 0.5 standard deviations σ of the amplitude distribution measured from the drive and response data set respectively. Without additive noise, the continuity measure is far more sensitive to weak coupling in this system than is cross correlation (we note the solitary case of poor continuity detection for zero noise at very weak coupling). However, as noise increases, cross correlation becomes a more robust determinate of coupling in this nonlinear system.

To demonstrate whether two ensembles of neurons from the brain are coupled, we record from simultaneously im-
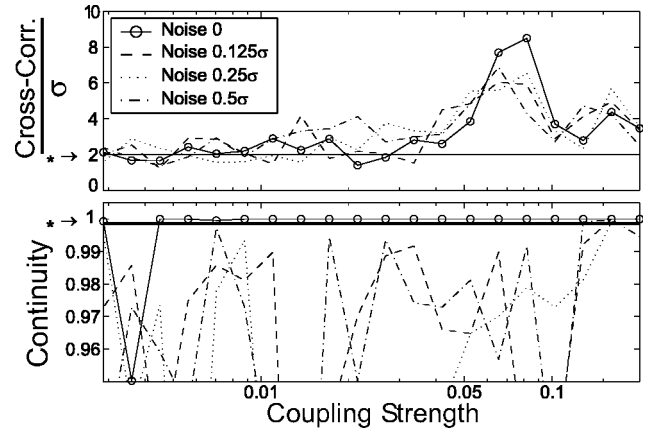

FIG. 3. Sensitivity of cross correlation vs continuity as a function of coupling strength and additive noise between Hénon systems. Continuity is more sensitive for the noiseless nonlinear case, but cross correlation is far more robust at all levels of additive noise. Asterisk (∗) indicates statistical confidence limits.

paled neurons within a live neuronal network, each from within separate neighborhoods of neurons. We turn off the spike generating mechanism in the impaled neurons in order to use them as receivers of inputs from their respective neighborhoods, then test whether the received signals are related. Rat brain slices were prepared as in Ref. [11]. Simultaneous intracellular voltage measurements from two neurons were recorded using whole cell patch clamp. Action potentials were suppressed by hyperpolarizing, permitting accurate measurement of the input synaptic currents. Coupling was measured under two conditions that altered the functional relationship between the neurons: slices bathed in normal $(3.5 \text{ m}M[\text{K}^+])$ versus mildly elevated potassium concentration $(5.5 \text{ m}M[\text{K}^+])$. This elevation in extracellular potassium causes a small increase in neuronal coupling [11].

Figure 4 illustrates the voltage recordings from two neurons as a function of low and high $[\text{K}^+]$. Time delay embedding lags were determined from the decay of the mutual information between the embedded time series as a function of lag [12]. Lag selected was the minimum integer value causing decay of the mutual information to $1/e$ of its value at 0 lag. Without knowledge of the underlying dynamics of the neuronal data, we tested for continuity at a range of embedding dimensions d showing data for $d = 1$, 2, and 3 in the figure.

The low $[\text{K}^+]$ condition is associated with no evidence of substantial coupling, in either cross correlation or continuity (Fig. 4, left). At the higher $[\text{K}^+]$ level, these neurons are more heavily coupled within the network, and cross correlation is significant (Fig. 4, right). In addition, continuity in elevated $[\text{K}^+]$, both forward and inverse, is significant at $d = 1$ and 3 (Fig. 4, right). In this neuronal network, we do not know (and cannot determine) the full nature of functional relationship between the neurons. Nevertheless, our finding of significant continuity establishes that these two neurons are functionally related, implying a common dynamical link.

An unknown balance between noise and nonlinearity in systems where an accurate model of the underlying equations is lacking may render it impossible to rely upon either
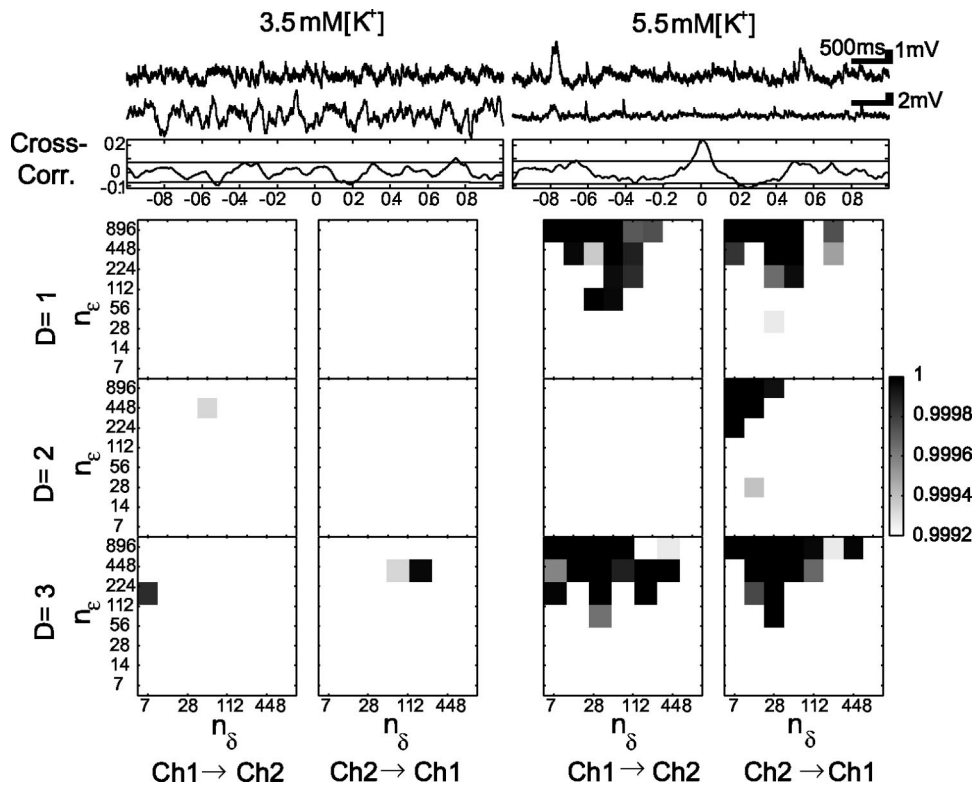
FIG. 4. Simultaneously measured intracellular voltages from two neurons as a function of low, left, and high, right, $[K^+]$ levels. No evidence of significant coupling, linear or nonlinear, is observed in low $[K^+]$, but evidence for both cross correlation and continuity (forward and reverse) is observed in high $[K^+]$. Gray scale as in Fig. 2.

global linear or local nonlinear methods alone to test for coupling between systems. We propose that a balanced approach to coupling identification in such systems is required, and will expand on these findings in a more detailed report [13]. By using these two methods with contrasting assumptions we have covered the whole of Fig. 1. We speculate that the question mark in the noisy nonlinear quadrant in Fig. 1 might be a global linear approach such as cross correlation, but this remains to be proven. Most importantly, we have elevated the continuity statistic beyond the usual *ad hoc* definitions requiring massive numerical work to gain statistical significance to an analytical level on par with the cross correlation where significance can be calculated directly.

[1] K. MacLeod and G. Laurent, Science **274**, 976 (1996).

[2] C.M. Gray, Neuron **24**, 31 (1999); F. Varela, J.P. Lachaux, E. Rodriguez, and J. Martinerie, Nat Rev Neurosci. **2**, 229 (2001).

[3] M.S. Bartlett, J. R. Stat. Soc. Ser. B. Methodol. **8**, 27 (1946); G.E.P. Box and G.M. Jenkins, *Time Series Analysis : Forecasting and Control* (Holden-Day, San Francisco, 1976).

[4] J. Theiler, S. Eubank, A. Longtin, B. Galdrikian, and J.D. Farmer, Physica D **58**, 77 (1992).

[5] L.M. Pecora, T.L. Carroll, and J.F. Heagy, Phys. Rev. E **52**, 3420 (1995).

[6] D.T. Kaplan, Physica D **73**, 38 (1994).

[7] J.T. Francis *et al.*, Physica D **148**, 175 (2001).

[8] S.J. Schiff *et al.*, Phys. Rev. E **54**, 6708 (1996).

[9] N.F. Rulkov *et al.*, Phys. Rev. E **51**, 980 (1995); J. Arnhold *et al.*, Physica D **134**, 419 (1999); C.L. Goodridge, L.M. Pecora, T.L. Carroll, and F.J. Rachford, Phys. Rev. E **64**, 026221 (2001).

[10] W. Feller, *An Introduction to Probability Theory and its Applications* (Wiley, New York, 1967); N. L. Johnson and S. Kotz, *Urn Models and Their Application* (Wiley, New York, 1977).

[11] T.I. Netoff, S.J. Schiff, J. Neurosci. **22**, 7297 (2002).

[12] A.M. Frazer and H.L. Swinney, Phys. Rev. A **33**, 1134 (1986).

[13] T. I. Netoff, S. J. Schiff, and L. M. Pecora (unpublished).